J Mater Sci (2007) 42:948–957
DOI 10.1007/s10853-006-0014-y

The impact properties and damage tolerance and of bi-directionally reinforced fiber metal laminates

Guocai Wu · Jenn-Ming Yang · H. Thomas Hahn

Received: 12 December 2005 / Accepted: 15 March 2006 / Published online: 11 January 2007

Abstract Fiber metal laminates are an advanced hybrid materials system being evaluated as a damage tolerance and light weight solution for future aircraft primary structures. This paper investigates the impact properties and damage tolerance of glass fiber reinforced aluminum laminates with cross-ply glass prepreg layers. A systematic low velocity impact testing program based on instrumented drop weight was conducted, and the characteristic impact energies, the damage area, and the permanent deflection of laminates are used to evaluate the impact performance and damage resistance. The post-impact residual tensile strength under various damage states ranging from the plastic dent, barely visible impact damage (BVID), clearly visible impact damage (CVID) up to the complete perforation was also measured and compared. Additionally, the post-impact fatigue behavior with different damage states was also explored. The results showed that both GLARE 4 and GLARE 5 laminates have better impact properties than those of 2024-T3 monolithic aluminum alloy. GLARE laminates had a longer service life than aluminum under fatigue loading after impact, and they did not show a sudden and catastrophic failure after the fatigue crack was initiated. The damage initiation, damage progression and failure modes under impact and fatigue loading were characterized and identified with microscopy, X-ray radiography, and by deply technique.

G. Wu (✉) · J.-M. Yang · H. T. Hahn
Department of Materials Science and Engineering,
University of California, Los Angeles, CA 90095, USA
e-mail: guocaiwu@ucla.edu

Present Address:
G. Wu
Cummins Inc., Columbus, IN 47201, USA

H. T. Hahn
Department of Mechanical and Aerospace Engineering,
University of California, Los Angeles, CA 90095, USA

Introduction

Fiber-reinforced metal laminates (FML) are hybrid composites consisting of alternating thin layers of metal sheets and fiber-reinforced resin prepreg. Due to its outstanding fatigue resistance, reduced density, high specific static properties, excellent impact resistance, it offers the structural designer a damage-tolerant, light-weight and cost-effective replacement for conventional aluminum alloy sheets or composites in advanced transport structural applications such as aircraft primary and secondary structures and blast-resistant luggage containers [1–5]. More recently, the FML with high strength S-2 glass fibers (tradename GLARE) has been selected for the upper fuselage skin structures of Airbus A380. However, the full potential of GLARE for primary aircraft structures has not been fully explored yet. More research and testing are necessary to generate adequate data for materials selection and design to develop predictive models and certification methodology to facilitate greater utilization of FML. One of important safety issues is the impact performance, damage tolerance and durability after impact for transportation structural applications, especially for airworthiness of FML as aircraft structures. Impact damage is unavoidable in aircraft structures because there are a lot of impact sources such as collisions

between service cars or cargo and the structure, dropped tools during maintenance, runaway debris, hail, and even bird strikes, etc. Previous researches [6–11] have demonstrated that fiber metal laminates (FML) are not so susceptible as the traditional composites to the formation of extensive internal damage under impact loading, and offer improved fracture toughness and comparable damage tolerance over the monolithic metallic materials.

Vlot et al. [6, 7] conducted the early extensive studies and compared the low and high velocity impact response of aramid fiber reinforced laminates (ARALL) and GLARE-1 with unidirectional prepreg layers and GLARE-3 with a cross-ply prepreg layers to monolithic aluminum and carbon-fiber-reinforced PEEK. The results illustrated that GLARE laminates have a superior impact resistance compared with ARALL, supposedly ''tough'' carbon-thermoplastic composites and monolithic aluminum alloy, especially under high velocity impact loading. Cantwell et al. [8] investigated the impact perforation resistance of a thermoplastic (polypropylene) based fiber metal laminates, and it clearly showed that it is superior to both monolithic aluminum and thermoset-based counterparts. Laliberte et al. [9] performed the impact response and post-impact fatigue behavior of GLARE compared with monolithic 2024-T3 aluminum. Lawcock et al. [11] studied the effect of varying fiber/matrix adhesion on the impact properties of a carbon fiber reinforced aluminum laminates and showed that laminates with lower levels of surface treatment exhibited increased amounts of fiber/matrix splitting and offered superior residual tensile properties.

Although the impact performance of fiber metal laminates has been evaluated extensively in recent years, there is still very little and insufficient information available in published literature, especially for GLARE laminates with bi-directional cross-ply S2-glass prepreg layers. Therefore, more in-depth studies are necessary to evaluate the impact performance, damage initiation and progression, damage tolerance and durability of GLARE laminates. This paper explores the impact properties and damage tolerance and durability of GLARE laminates with newly cross-plied prepreg layers. A broad impact testing program was performed, and the results were compared with those obtained on monolithic aluminum counterparts. The impact damage was characterized, and the damage mechanism was analyzed and discussed. The post-impact residual strength and post-impact fatigue under various damage states was extensively investigated.

Experimental procedures

Materials

The fiber metal laminates used in the present experimental investigation are GLARE 4-3/2 and GLARE 5-2/1 provided by Aviation Equipment, Inc (Costa Mesa, CA). GLARE 4-3/2 consists of three layers of 2024-T3 aluminum alloy sheets and two layers of 0°/90°/0° glass-reinforced epoxy prepreg with 67% fiber in 0° direction and 33% fiber in 90° direction. GLARE 5-2/1 laminates consist of two layers of 2024-T3 aluminum alloy sheet with one layer of 50/50 glass-reinforced epoxy prepreg with 0°/90°/90°/0° fiber orientation. The average thickness of each layer for the as-received GLARE laminates was measured using optical micrographs. The average thickness of GLARE 4-3/2 was measured to be 0.304 mm for aluminum alloy sheets and 0.458 mm for prepreg layers. The average thickness of GLARE 5-2/1 was 0.489 mm for aluminum layers and 0.584 mm for prepreg layers. Therefore the actual average thickness of GLAR4-3/2 and GLARE 5-2/1 laminate in the present study are 1.828 and 1.562 mm, respectively. The monolithic 2024-T3 aluminum alloy with a thickness of 1.60 mm was also used as a baseline material for comparison.

Test procedures

All impact tests were performed using a Dynatup Model 8250 instrumented drop weight impact tower equipped with a pneumatic rebound brake system and with a maximum impact velocity of 13.4 m/s. A PC based data acquisition system GRC 930-I, supplied by Dynatup, triggered by a photo diode velocity detector just prior to impacting the specimen was used to collect data. Immediately upon impact, the pneumatic rebound breaks are activated to push up and hold the impactor assembly in place so that the specimen is not subjected to multiple impacts. The impact testing specimens were cut from 300×300 mm GLARE panels. The square specimens with a size of 76×76 mm^2 were clamped between two steel plates with a 50×50 mm^2 circular central opening in the impact fixture. A spherical steel impactor of 12.7 mm in diameter was used and impactor mass was 6.29 kg. Various impact energies ranging from 7 to 40 J were achieved by adjusting the dropping height during low velocity impact tests. Four specimens were tested for each height. The specimens were impacted at various energy levels resulting in damage that varied from small indentation to complete penetration. After impact the specimens were then carefully removed

for inspection and characterization of damage states. The specimens under different impact energies were then sectioned through the mid-plane of the impact location and polished to observe the damage patterns. The impact energy at which first visible crack at the surface of outer aluminum layer is formed, was taken as a critical value (minimum cracking energy). The perforation is defined as the complete piercing by the impactor. The impact damage resistance is quantified by the two characteristic energy values, minimum cracking energy and perforation energy, together with the permanent deflection depth and damage area in the glass/epoxy layer.

The residual strength after impact was used to evaluate the impact damage tolerance. The specimens for residual strength tests were 305 mm long and 75 mm wide, and were subjected to low-velocity impact with the same set-up described above. Five impact energies were chosen for residual strength tests to create a scope of damage states ranging from barely visible impact damage (BVID), clearly visible impact damage (CVID) to complete penetration.

The post-impact tension–tension fatigue tests were performed on a computer-controlled servohydraulic Instron system. All tests were conducted at a stress ratio of 0.1 and a frequency of 10 Hz under a load-controlled mode. The maximum applied stresses were chosen to be 20, 30, 40, 50, 60% of residual strength of each laminates. Three impact damage states ranging from dent (BVID), cracking (CVID) up to complete penetration were selected. Two specimens were measured in each testing condition. The initiation and propagation of fatigue cracks were monitored using cellulose acetate replicating tapes that were pasted on the specimen by acetone solution. Fatigue crack length data was collected for all post-impact specimens at 5,000 or 10,000 cycle intervals.

Results and discussion

Impact performance of GLARE laminates

A number of specimens were impacted at different energies for GLARE5-2/1, GLARE4-3/2 and bare 2024-T3 aluminum. The first failure was observed as a visible crack in the outer aluminum layer at the non-impacted side of GLARE laminates due to bending deformation. As the impact energy increased, failure occurred at the impacted-side of aluminum layer, and then a through crack was created with further increasing impact energy. The energies required to create a first cracking and perforation are given in Table 1. The measurement error in minimum cracking and perforation energy was within 0.2 J. It is shown that the perforation energy for both types of GLARE laminates is higher than that for monolithic aluminum. Due to the effect of different laminate thickness on characteristic energies, the thickness correction was introduced to compare the damage initiation energy and penetration energy of conventional composite laminates [12–14]. For fiber-metal laminates, Vlot [6, 7] and Compston [8] took a similar step and they related the impact energy to weight through the evaluation of specific energy; the ratio of impact energy to the areal density of the specimen. The same approach is taken in the present study. Figure 1 shows a comparison of the impact energy needed to create the first cracking and perforation of different materials on a specific basis. It is shown that both types of GLARE laminates exhibit a high impact damage resistance and GLARE 5-2/1 is slightly better than GLARE 4-3/2 laminate. The specific energy needed to create a visible crack in the

Table 1 Minimum cracking energy and perforation energy for GLARE laminates

Materials	Thickness (mm)	Areal density (kg/m^2)	Minimum cracking energy (J)	Perforation energy (J)
2024-T3 aluminum	1.6	4.45	18.1	33.4
GLARE 5-2/1	1.562	3.74	16.3	34.5
GLARE 4-3/2	1.828	4.23	13.9	38.3

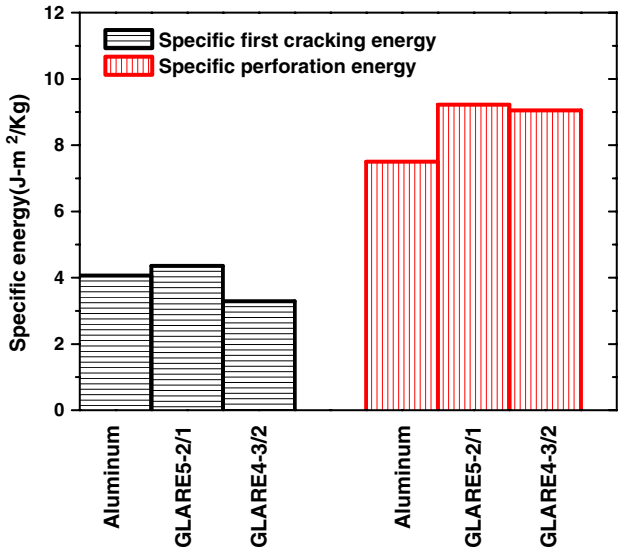

Fig. 1 Specific characteristic energies for different materials at low velocity impact

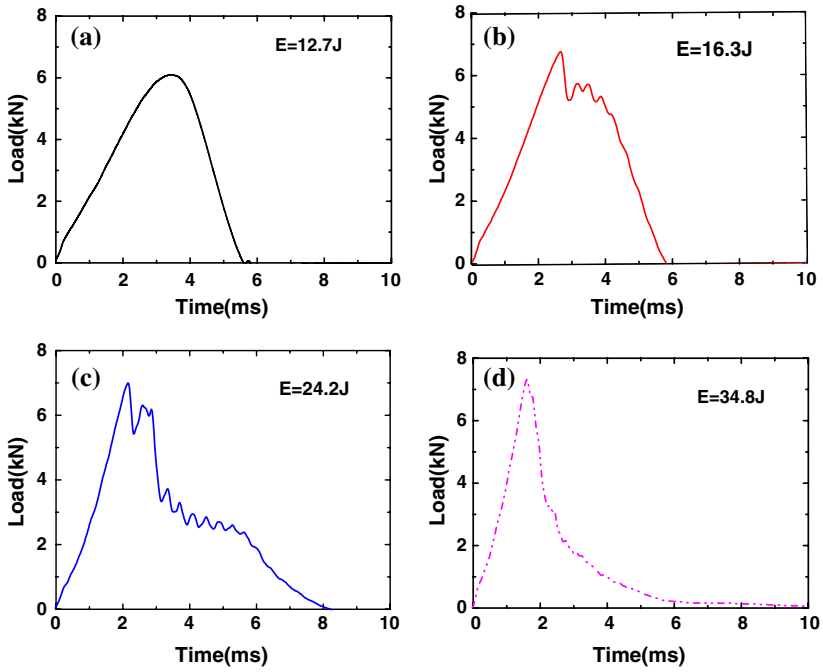

Fig. 2 Load–time histories of GLARE 5-2/1 laminate under low velocity impact energies

outer aluminum layer at the non-impacted side for GLARE 5-2/1 laminate is higher than both GLARE 4-3/2 laminate and monolithic aluminum. Also, the specific perforation energy for both GLARE laminates is higher than that for monolithic aluminum.

Figure 2 shows a typical load–time history of impact tests for GLARE 5-2/1 laminate. It can be seen that the load vs. time curve is rather smooth under the 12.7 J of impact energy indicating that only plastic indentation occurred. First cracking in the outer aluminum layer at the non-impacted side is indicated by a sharp load drop under the 16.3 J of impact energy. The discrete load drops in the curve after first cracking indicates the delamination and failure of other layers. At an impact energy of 34.5 J, the load was dramatically reduced indicating the occurrence of full penetration. A similar behavior was observed for GLARE 4-3/2 laminate as shown in Fig. 3.

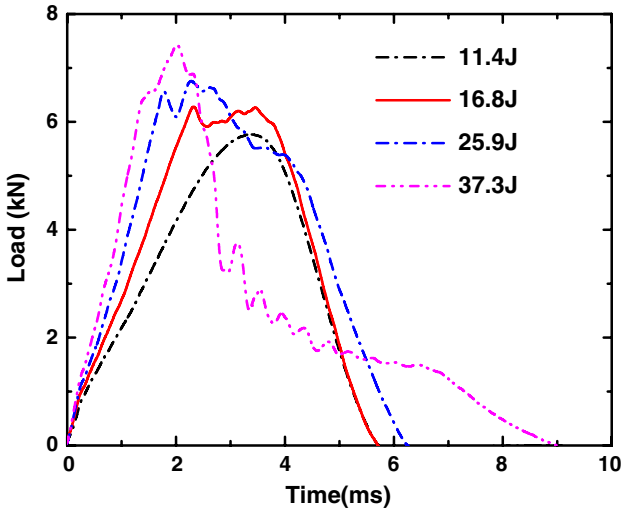

Fig. 3 Load–time histories for GLARE 4-3/2 laminate under different impact energies

Impact damage characterization and failure mechanism

The low velocity impact-induced damage in the GLARE laminates can be divided into two categories: visible damage in the form of local plastic indentation and internal damage such as fiber failure, matrix cracking and delamination. The results of specimens after testing showed that GLARE laminates with different fiber orientations and stacking sequences exhibited distinctive features of both impact deformation and cracking. For GLARE 5 laminate and bare aluminum, a spherical-shaped permanent plastically deformed dent was observed on the surface of the outer aluminum layer at the non-impacted side around the point of impact. In contrast, an elliptical configuration with a major axis along the 0° fiber reinforcement direction was observed for GLARE-4 laminate. Figure 4 shows the typical visible damage mode for GLARE laminates. GLARE-5 exhibits cracking in the outer aluminum layer at the non-impacted side in both 0° and 90° directions, however, GLARE-4 cracks along the 0° fiber direction, and the crack was centered

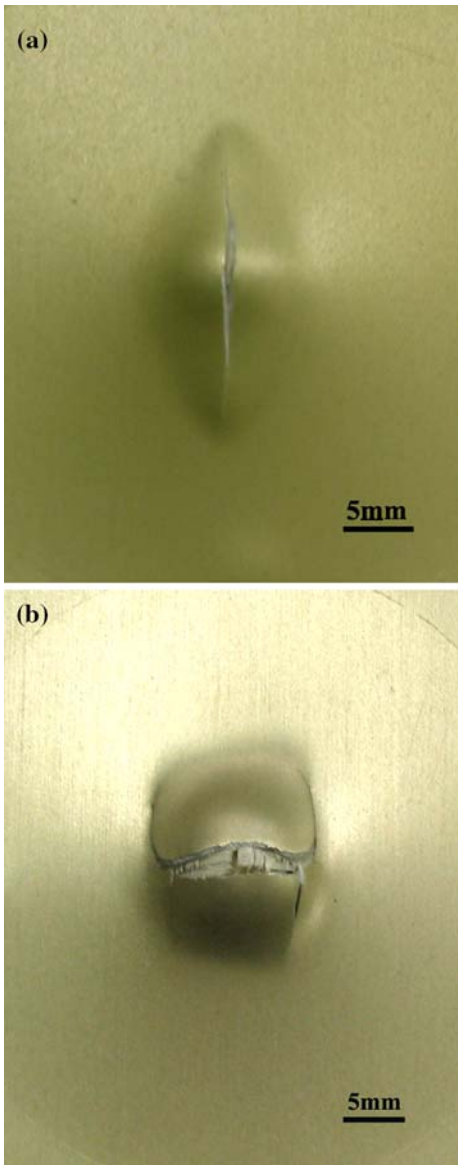

Fig. 4 Visible damage mode in the outer aluminum layer at the non-impacted side of GLARE laminates (**a**) GLARE 4-3/2; (**b**) GLARE 5-2/1

within the dent. It is interesting to note that a stable impact crack growth behavior in outer aluminum layer at the non-impacted side was found up to the impact energy of 28 J for GLARE-4 laminate. Over this impact energy, the crack slightly branched into 90° fiber direction at the edge of elliptical dent of GLARE-4 laminate. Subsequently the specimen was penetrated with the further increasing impact energy.

The internal damage mode of GLARE 5-2/1 was shown in Fig. 5. At 12.7 J, no visible crack in the outer aluminum layers was found except permanent deformation around the point of impact. However, there is considerable delamination between the non-impacted

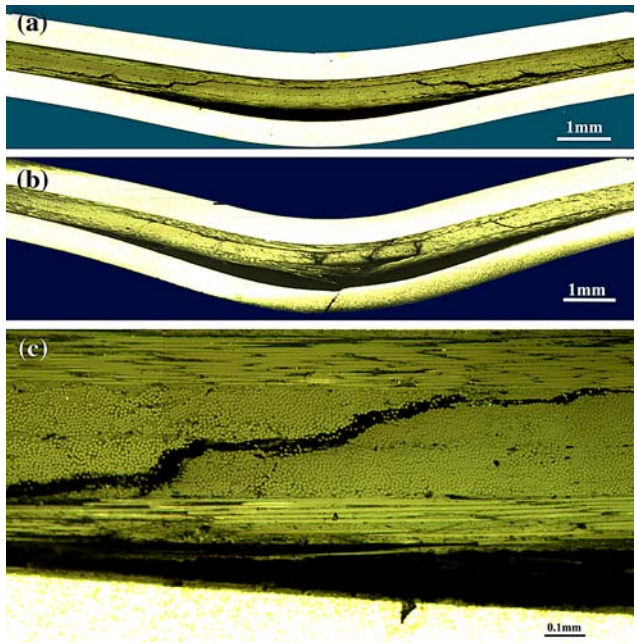

Fig. 5 Internal impact damage mode in the GLARE 5-2/1 laminate (**a**) at an impact energy of 12.7 J; (**b**) at an impact energy of 16.3 J; (**c**) A highlight of damage in the composite layer of GLARE 5-2/1 laminate subjected to an impact energy of 12.7 J

aluminum layer and composite layer as shown in Fig. 5a. This suggests that interfacial shear stresses due to bending had caused debonding at the aluminum–composite interface. The delamination allows GLARE laminates to deform and fracture in a more efficient membrane way, and it contributes to total energy absorption [7, 8]. In addition, the composite layer exhibits extensive microcracking and intra-delamination between 0° fiber and 90° fiber ply. And the matrix cracking within the 90° plies is inclined at approximately 45° indicating the influence of transverse shear stresses. Similar observation was found in traditional laminated composites containing different ply orientations under low velocity impact [15–17]. When the 45° matrix crack is initiated and propagated to the interface between 0° and 90° ply, it is unable to penetrate to 0° fiber layer and thus the intra-delamination is created at the interface between 0° and 90° fiber ply within the composite layer. The micrograph of samples subjected to an impact energy of 16.3 J as shown in Fig. 5b. The damage includes the cracking in outer aluminum layer at the non-impacted side as well as extensive fiber fracture in the outermost 0° fiber layer, the matrix crack in the 90° fiber layer and intra-delamination between 0° and 90° fiber ply. As the impact energy increases, the damage became more severe, and there are more extensive fiber breakage and matrix cracks.

Ultimately, when the aluminum layer at impacted-side cracked, the laminate is perforated.

The damage zone in the glass/epoxy layer after chemically removing the outer aluminum layers, and the permanent impact deflection depth were also measured to evaluate the impact damage resistance and performance. The damage zone in the composite layer is roughly circular in shape for GLARE 5 laminate but the damage zone is elliptical for GLARE 4 laminate with the long axis oriented along 0° fiber direction as shown in Fig. 6. And it was found that the internal impact damage in GLARE laminates is mostly confined to a relatively small area surrounding the point of impact and the impact damage was always smaller than the size of the visible plastically deformed dent exposed at the outer aluminum layers for all GLARE specimens. This is beneficial to damage inspection. The damage area for both types of GLARE laminates is shown in Fig. 7. The size of the damage zone increases with increasing impact energy for both types of GLARE as expected. However, a considerably sharp increase in damage size was observed between around 22.1 J and 25.9 J for GLARE 5-2/1 and GLARE 4-3/2, respectively. This corresponds to the point at which the cracking occurs in the outer aluminum layer at the impacted side of GLARE laminates. The damage area continuously increases with increasing impact energy levels and it levels off until the full penetration. Figure 8 shows the permanent central deflection as a function of impact energy after low velocity impact. The GLARE laminates have approximately the same dent depth as monolithic aluminum after impact, and GLARE 5-2/1 laminate gives a slightly larger dent depth.

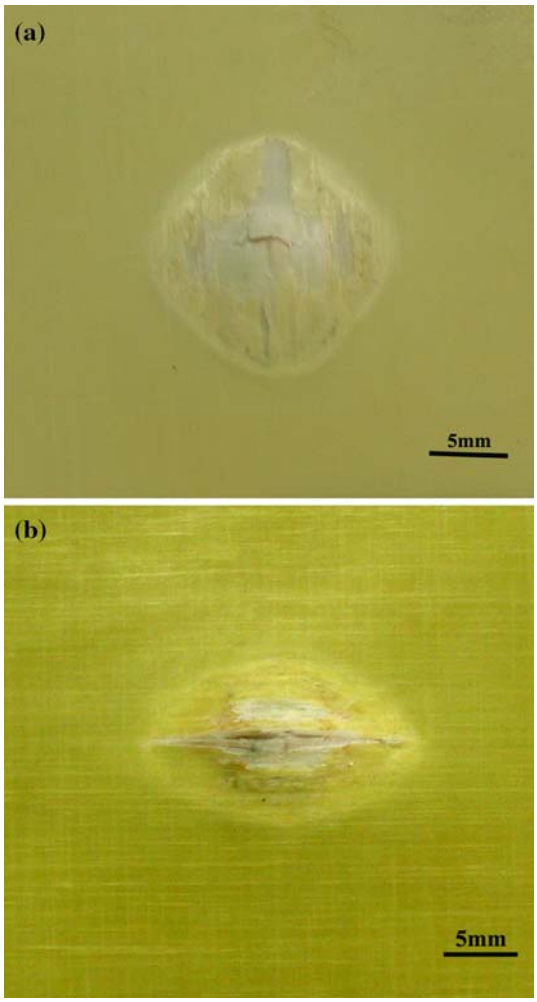

Fig. 6 Impact damage zone at 21.8 J after removal of outer aluminum layers (**a**) GLARE5-2/1; (**b**) GLARE4-3/2

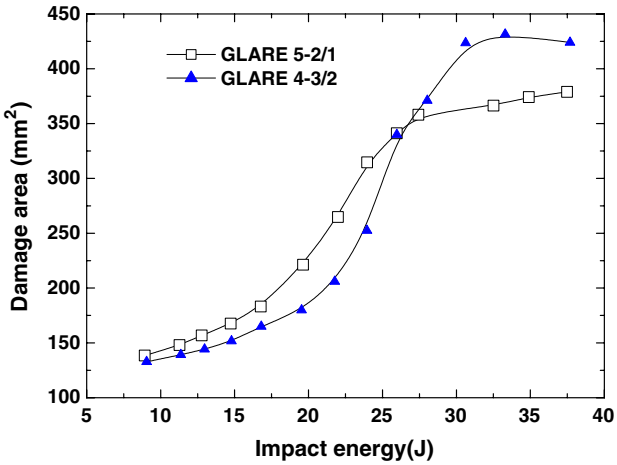

Fig. 7 The damage area as a function of the impact energy for GLARE laminates

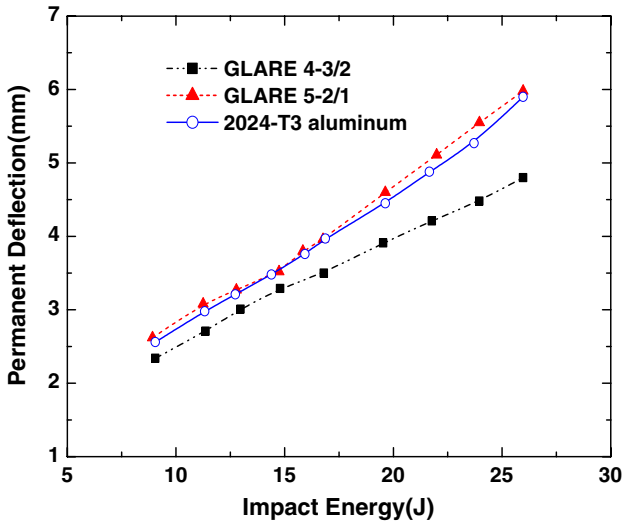

Fig. 8 The permanent central deflection as a function of the impact energy

Post-impact residual strength of GLARE laminates

The damage tolerance of a material is related to its residual strength in the presence of damage. Due to pronounced permanent deformation inflicted on the specimen after impact, compression tests are difficult to perform without global failure. Therefore, residual tensile tests were performed in the present study. The residual tensile strength after impact vs. impact energies is given in Fig. 9. There is a steady reduction in residual strength for both the GLARE 5 laminate and monolithic aluminum with increasing impact energy. Both GLARE 5-2/1 and aluminum retained about 50% of its strength after complete perforation. However, the residual tensile strength of GLARE 5-2/1 was about 322 MPa, which is higher than that for aluminum. At the impact energy of 10.8 J, only local plastic dent (BVID) was found in both GLARE 5-2/1 and aluminum. Therefore, the strength reduction is very minor. It is obvious that the residual strength of GLARE 5 was not influenced much by the presence of the dent as in the monolithic aluminum. As the impact energy increased to 16.4 J, the residual strength decreased substantially. This is consistent with our microscopic damage observation that clearly visible cracking (CVID) occurred at the non-impacted aluminum layer in GLARE 5 and in monolithic aluminum. With the continuing increase of impact energy, the residual strength decreased continuously. However, the reduction in residual strength for monolithic aluminum is more severe than that for GLARE. This is attributed to the glass fiber bridging effect of GLARE laminates at the front of the damage zone. So, the stress intensity factor at the crack tip of outer aluminum layers is reduced, and the crack propagation in the outer aluminum layers is postponed. At the impact energy of 23.7 J, cracking in the outer aluminum layer at the impacted side appeared in GLARE laminates along with the fiber failure and extensive matrix cracking. This resulted in further reduction of residual tensile strength of the GLARE 5 laminate.

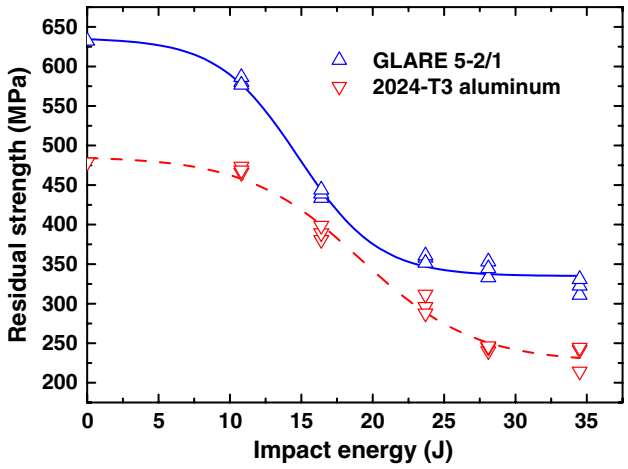

Fig. 9 Post-impact residual strength of GLARE under different damage states

Post-impact fatigue behavior of GLARE laminates

Constant amplitude tension–tension fatigue testing was performed to investigate the durability of GLARE laminates to retain its structural performance with impact damage. Table 2 shows the fatigue test results of GLARE laminates at the maximum stress of 232.4 MPa with a dent inflicted by an impact energy of 10.8 J. Few specimens showed a premature fracture and failed in the gripping region because of high stress concentration in the tab, but most of specimens failed in the dent region. For all GLARE 4-3/2 and GLARE 5-2/1 specimens, the fatigue crack initiated at the edge of concave dent, and then slowly propagated to the edge. For GLARE 5-2/1, the specimen was not ruptured immediately and survived thousands of cycles even though the crack already reached the edge. However, for GLARE 4-3/2, multiple cracks appeared around the dent regions at both concave and convex sides after the fatigue crack reached the edge of specimen, which resulted in a long fatigue life cycles as shown in Table 2. For the monolithic aluminum, the

Table 2 Summary of post-impact fatigue test results

Specimen	Cycles to initiation	Cycles to reach edge	Cycles to failure	Comments
Aluminum	37,639		37,889	Failed suddenly
Aluminum	34,472		35,556	Failed suddenly
GLARE5	18,828	36,089	42,188	Crack initiated at the edge of concave dent, and then crack propagated to the edge
GLARE4	17,813		125,030	Crack initiated at the edge of concave dent, but failed inside grip region
GLARE4	20,775	136,775	371,775	Crack initiated at the edge of concave dent and propagated to the edge, and then multiple crack appeared until failure

failure suddenly occurred after the fatigue cracking initiated at the edge of dent. Although aluminum have longer crack initiation cycles than GLARE laminates, the fatigue cycles for crack propagation in GLARE laminates is much higher than aluminum, especially in GLARE 4. One of GLARE 4 specimens failed at 372,775 cycles, which is an order of magnitude higher than aluminum.

Figure 10 presents the fatigue crack growth curves as function of fatigue cycles for GLARE 4. It is obvious that GLARE 4 exhibited a slow and stable fatigue crack growth after impact loading. The fatigue crack growth rate is almost constant after fatigue crack was initiated. Figure 11 clearly illustrated the post-impact fatigue crack progression with the fatigue cycles in GLARE 4. Fatigue crack did not reach the edge even at 80,000 fatigue cycles.

After impact, a complicated residual stress system is present surrounding the impact site [6]. On the impacted (concave) side, the tensile stress existed within the dent. On the non-impacted (convex) side, the compressive stress was induced within the dent due to spring back while the residual tensile stress existed surrounding the dent. When the impacted specimen with the dent is subjected to overall tensile loading as in the present fatigue study, tensile strain was induced in the heavily deformed region at the edge of the dent on the non-impacted side. That is why the fatigue crack in GLARE laminates was first initiated at the edge of the dent of the non-impacted side. As the fatigue crack in the aluminum layer progressed, stress was transferred onto the prepreg layers due to glass fiber bridging effect. The fiber bridging retards the fatigue crack growth. When the growth of fatigue crack reached the edges of the specimen, it did not lead to catastrophic failure because the prepreg layers had sufficient residual strength to carry the fatigue loads. Compared with the sudden failure of aluminum, this is very beneficial to periodic inspection and maintenance of aircraft structures.

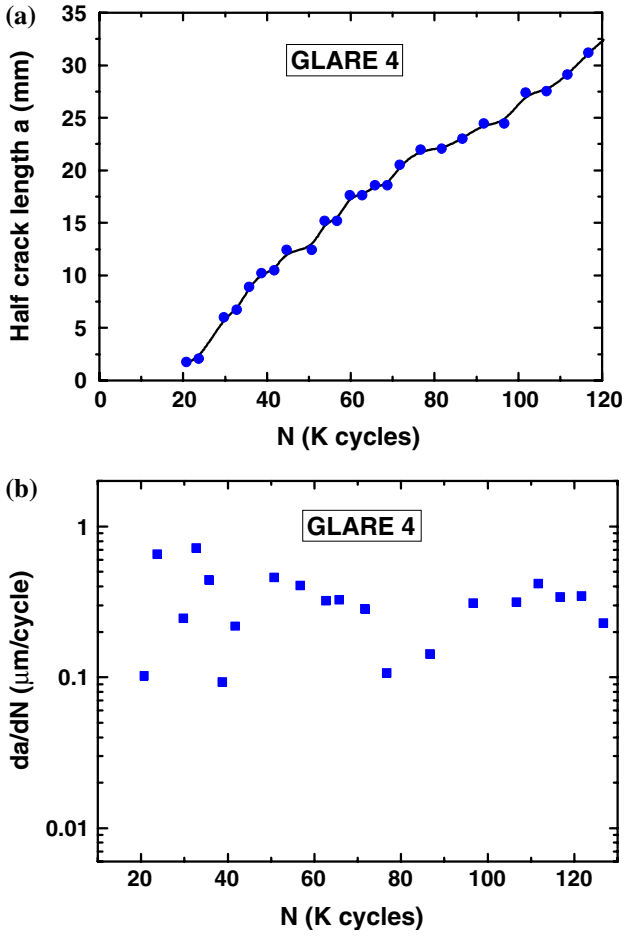

Fig. 10 Post-impact fatigue behavior of GLARE 4 laminate (**a**) half crack length as a function of fatigue cycle; (**b**) crack growth rate as a function of fatigue cycle

Summary

The low velocity impact performance and damage tolerance of glass fiber reinforced aluminum laminates with cross-ply S2-glass prepreg have been investigated. The quantitative results on specific energies, damage area, and permanent deflection revealed that both GLARE 4 and GLARE 5 laminates have improved impact properties than those of 2024-T3 monolithic aluminum alloy. The energy to create a visible crack in the outer aluminum layer at the non-impacted side for GLARE 5-2/1 laminate is higher than both GLARE 4-3/2 laminate and monolithic aluminum on the specific weight basis. The specific perforation energy for both GLARE laminates is higher than that for aluminum alloys.

GLARE 5-2/1 exhibited cracking in both 0° and 90° directions at the outer aluminum layer, but GLARE 4-3/2 cracked along the major fiber direction. The damage zone is roughly circular in shape for GLARE-5 laminates but it is elliptical for GLARE-4 laminate with the long axis oriented along 0° fiber direction. Besides the delamination at the aluminum–composite interfaces and fiber fracture, the microscopic investigation of internal damage mode also indicated the presence of extensive microcracking incline at approximately 45° and intra-delamination between 0° and 90° fiber plies. All these failure mechanisms combined with permanent plastic deformation and cracking in the thin aluminum layers contribute to outstanding impact energy absorption capability of GLARE laminates.

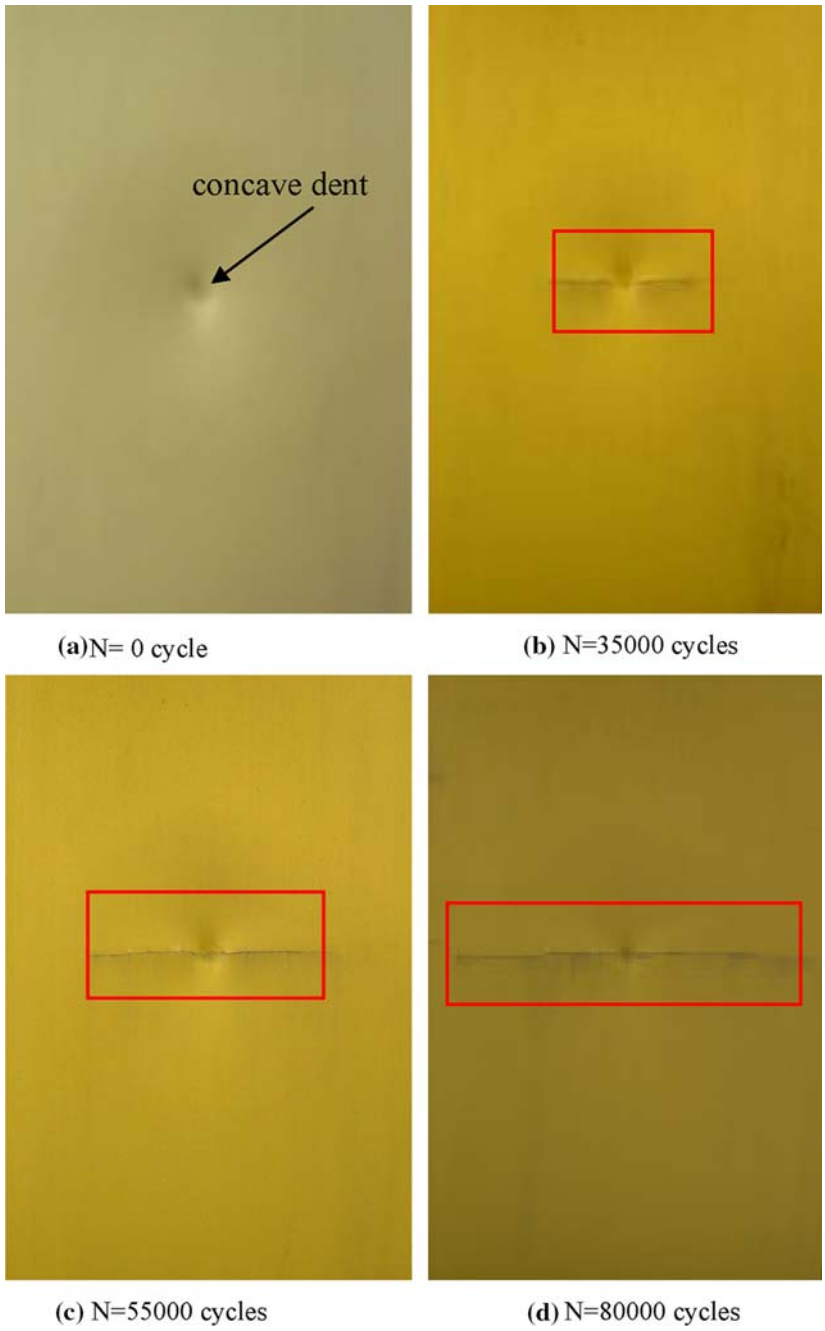

Fig. 11 Stable fatigue crack growth behavior of GLARE 4

And also visible plastically deformed dent and localized small internal impact damage surrounding the point of impact are beneficial to damage inspection.

The post-impact residual strength results showed that GLARE laminate had a higher impact damage tolerance than the monolithic aluminum alloys. The residual strength of the GLARE 5 laminate retained a higher residual strength than its aluminum counterpart at all impact damage states. GLARE laminates also showed a superior post-impact fatigue performance to aluminum. The fatigue failure in aluminum was sudden and catastrophic, but the fatigue crack was initiated at the edge of non-impacted outer aluminum layers and slowly propagated to the edge of specimens. GLARE laminates had a longer service life than aluminum under fatigue loading after impact.

Acknowledgements This work was supported by Federal Aviation Administration (FAA) through the Center of Excellence on Composites and Advanced Materials. Curt Davies is the program manager. The authors thank Mr Hyoungseock Seo for his participation in post-impact fatigue testing.

References

1. Vogeslang LB, Vlot A (2000) J Mater Process Technol 103:1
2. Vermeeren CAJR (2003) Appl Comp Mater 10:189
3. Vlot A, Vogelesang LB, de Vries TJ (1999) Aircr Eng Aerosp Technol 71:558
4. Afaghi-khatibi A, Ye L, Mai YW (2000) In: Comprehensive composite materials, vol 2, pp 249–290
5. Wu G, Yang J-M (2005) JOM 57(1):72
6. Vlot A, Kroon E, La Rocca G (1998) Key Eng Mater 141–143:235
7. Vlot A (1996) Int J Impact Eng 18:291
8. Compston P, Cantwell WJ, Jones C, Jones N (2001) J Mater Sci Lett 20:597
9. Laliberte JF, Poon C, Straznicky PV, Fahr A (2002) Int J Fatigue 24:249
10. Sun CT, Dicken A, Wu HF (1993) Comp Sci Technol 49:139
11. Lawcock GD, Ye L, Mai YW, Sun CT (1997) Comp Sci Technol 57:1621
12. Hwang B (1994) Damage initiation during low-velocity impact on composite laminates. PhD Dissertation, University of Dayton
13. Carlile DR, Leach DC (1983) In: Proceedings of 15th National SAMPE Technical Conf., Oct. 4–6, 1983, pp 82–93
14. Sykes GF, Stoakley DM (1980) In: Proceedings of the 12th National SAMPE Technical Conf., Oct. 7–9, 1980, pp 482–493
15. Choi HY, Wu H-YT, Chang FK (1991) J Comp Mater 25:992
16. Liu D, Malvern LE (1987) J Comp Mater 21:594
17. Joshi SP, Sun CT (1985) J Comp Mater 19:51